

Heterogeneous & Homogeneous & Bio- & Nano-

CHEM **CAT** CHEM

CATALYSIS

Accepted Article

Title: Al-doped SBA-15 catalysts for low-temperature dehydration of 1,3-butanediol into butadiene

Authors: Marc Pera-Titus, Fangli Jing, Benjamin Katryniok, Sebastien Paul, Lin Fang, Armin Liebens, Ming Shen, Bingwen Hu, and Franck Dumeignil

This manuscript has been accepted after peer review and appears as an Accepted Article online prior to editing, proofing, and formal publication of the final Version of Record (VoR). This work is currently citable by using the Digital Object Identifier (DOI) given below. The VoR will be published online in Early View as soon as possible and may be different to this Accepted Article as a result of editing. Readers should obtain the VoR from the journal website shown below when it is published to ensure accuracy of information. The authors are responsible for the content of this Accepted Article.

To be cited as: *ChemCatChem* 10.1002/cctc.201601202

Link to VoR: <http://dx.doi.org/10.1002/cctc.201601202>

WILEY-VCH

www.chemcatchem.org



Al-doped SBA-15 catalysts for low-temperature dehydration of 1,3-butanediol into butadiene

Fangli Jing,^[a,c] Benjamin Katryniok,^[a] Sébastien Paul,^[a] Lin Fang,^[b] Armin Liebens,^[b] Ming Shen,^[d] Bingwen Hu,^[d] Franck Dumeignil,^[a] and Marc Pera-Titus^{[b]*}

Abstract: SBA-15 doped with variable aluminum amounts were prepared through a facile evaporation-induced self-assembly process. The textural properties and the acidity of the catalysts could be simply tuned by the aluminum content. The genesis of acid sites with weak and medium strength during reaction was directly correlated to the catalytic activity for the dehydration of 1,3-butanediol into butadiene. The best performance was achieved over an Al-SBA-15 sample with a silica/alumina ratio of 76, exhibiting a stable BD yield of 59% at a temperature as low as 200 °C.

Fossil resources including coal, oil and natural gas give access directly or indirectly to almost all fuels, chemicals and materials used in our everyday life with an increasing demand due to the rapid growth of the world population.^[1] Obviously, the utilization of these finite resources cannot be a long-term policy, and more and more attention has been paid to the development of sustainable processes relying on biomass conversion into high-value added products.^[2]

As a paradigmatic example of an petroleum-derived intermediate, one can mention butadiene (BD), which is used for the synthetic rubber and resin industries.^[3] The current BD production processes rely on naphtha cracking and on the catalytic oxidative dehydrogenation of *n*-butane and *n*-butene, which are all non-sustainable feedstocks.^[4] Thus, it becomes urgent to design alternative routes for BD production using renewable materials. The Lebedev process has attracted much interest for BD production, since bioethanol can be used as starting raw material.^[5] This reaction is usually catalyzed over catalysts combining basic and acid sites, including the classical MgO/SiO₂,^[3c,6] and ZrO₂/SiO₂,^[3b,7] ZnO/γ-Al₂O₃,^[8] and ZnO/ZrO₂/SiO₂.^[3b]

As an alternative to the Lebedev process, butanediols (BDO) are competitive biobased substrates that can be derived from glucose, sucrose, glycerol and mixtures of glucose and xylose by fermentation.^[9] The dehydration of BDOs can lead to different chemicals depending on the starting diol and the catalyst used.^[10] Indeed, 1,2-BDO dehydration over ZnSO₄ in supercritical water yields *n*-butyraldehyde,^[11] whereas 1,3-BDO and

1,4-BDO dehydration over rare-earth and weak acid oxides (e.g., ZrO₂) at 300-500 °C affords unsaturated alcohols.^[12] Promising BD selectivities up to 42% and >90% at full 2,3-BDO conversion were recently reported over Al₂O₃ and Sc₂O₃ below 350 °C, respectively.^[13] Finally, HZSM-5 zeolites enriched with mild Brønsted acid sites yields mainly methyl ethyl ketone (MEK) upon 2,3-BDO dehydration,^[14] while BD could be achieved at 60% yield at 300-350 °C starting from 1,3-BDO.^[15] Here, Al-doped SBA-15 samples were prepared as proto-typical acid catalysts using the evaporation-induced self-assembly (EISA) method and calcined under air at 550 °C (see SI for experimental details).^[16] The catalysts were denoted as SBA@X, where X indicates the bulk SiO₂/Al₂O₃ ratio measured by X-ray fluorescence (XRF) (Table S1). Most of the Al species segregated on the silica mesostructure and accordingly were not integrated into the silica framework as inferred from the much larger SiO₂/Al₂O₃ surface ratios (XPS) compared to bulk SiO₂/Al₂O₃ ratios (XRF) (Table S2). The samples were further used for catalyzing the gas-phase dehydration of 1,3-BDO towards BD.

The SBA@X catalysts showed regular type IV N₂ isotherms with symmetric H1-type hysteresis loops according to the IUPAC classification (Figure S1A), indicating the presence of cylindrical and independent mesopores.^[17] The hysteresis loop evolved from *P*/*P*₀ = 0.40-0.62 for SBA@250 to *P*/*P*₀ = 0.40-0.80 for SBA@27, reflecting broader pore size distributions (BJH) in the range 3-6 nm (Figure S1B). Likewise, the BET specific surface area increased inversely with the Al content from 492 m²/g for SBA@27 to 688 m²/g for SBA@250 with ca. 20% of the surface microporosity (Table 1, Figure S2). Such a trend was still found on the catalysts after reaction at 300 °C for 8 h, even if the surface areas dropped significantly by 45-53% and the contribution of microporosity declined below 10% for samples SBA@190, SBA@102 and SBA@76. Notwithstanding this fact, the main porous features of the catalysts were preserved (especially at SiO₂/Al₂O₃>76) without any qualitative change on the N₂ sorption patterns (Figure S1C-D). The textural changes can be attributed to coke formation as confirmed by TGA-MS and XPS (Table 1, Table S2, Figure S3). Lower carbon (86 mgC/g) was generated over SBA@190, whereas 111-119 mgC/g was obtained over SBA@102, SBA@76 and SBA@27.

The total amount and distribution of acid sites on the fresh and spent SBA@X catalysts was measured by NH₃-TPD in the temperature range 100-1000 °C (Table 2, Figure 1 - blue curves, Figure S2, S4). In this analysis, we assumed that all the hydroxyl groups that could be titrated by NH₃ corresponded to bridged Si-OH-Al sites, but not to weakly acid Si-OH groups far from Al centers. Two distinctive NH₃ desorption bands could be discerned in the fresh SBA@X catalysts: (1) weak acid sites in the range 100-240 °C (LT), and (2) strong acid sites in the range 240-1000 °C (HT). Interestingly, qualitatively similar NH₃-TPD patterns were observed on Al-SBA samples prepared

[a] Dr. F. Jing, Dr. B. Katryniok, Prof. S. Paul, Prof. F. Dumeignil
Univ. Lille, Univ. Artois, CNRS, ENSCL, Centrale Lille, UMR 8181 -
UCCS - Unité de Catalyse et Chimie du Solide
Bd. Paul Langevin, 59000 Lille, France

[b] Dr. A. Liebens, Dr. M. Pera-Titus
E2P2L UMI 3464 CNRS/Solvay
3966 Jin Du Road, 201108 Shanghai, China.
Email: marc.pera-titus-ext@solvay.com

[c] Dr. F. Jing
School of Chemical Engineering
Sichuan University
No. 24, South section 1, Yihuan Road, 610065 Chengdu, China

[d] Mr. M. Shen, Dr. B. Hu
School of Physics and Materials Science & Shanghai Key Laboratory of
Magnetic Resonance
East China Normal University
3663 N. Zhongshan Road, Shanghai 200062, China

Supporting information for this article is given via a link at the end of the document.

either by direct synthesis ($\text{SiO}_2/\text{Al}_2\text{O}_3 = 20\text{-}100$),^[18] or by post-synthesis Al grafting over SBA-15 ($\text{SiO}_2/\text{Al}_2\text{O}_3 = 38\text{-}130$).^[19] However, while the LT bands on those catalysts matched the temperature range observed on our SBA@X catalysts, the (deconvoluted) HT bands appeared at comparatively lower temperatures (240-600 °C), reflecting in our case the genesis of stronger acid sites. The density of weaker sites in the SBA@X catalysts was very sensitive to the $\text{SiO}_2/\text{Al}_2\text{O}_3$ ratio, varying monotonously from 15 $\mu\text{mol/g}$ for SBA@250 to 186 $\mu\text{mol/g}$ for SBA@27. In contrast, by comparing the NH_3 loadings on strong acid sites with the total Al loadings, abnormally high NH_3 loadings were measured (Table 2). This observation can be explained by the formation of $\text{NH}_4^+ \cdot n\text{NH}_3$ associations on strong Brønsted acid sites, with n decreasing with the $\text{SiO}_2/\text{Al}_2\text{O}_3$ ratio until 0.8 for SBA@27.^[20] Furthermore, partial conversion of Lewis into Brønsted acid sites during NH_3 adsorption and further TPD tests cannot be ruled out.^[21]

The NH_3 -TPD profiles were also measured on the spent SBA@X catalysts after calcination at 500 °C to remove the deposited carbon according to the TGA-MS profiles (Figure 1 - red curves, Figure S3). Two LT and HT bands ascribed to weak and strong acid sites, respectively, were also observed. Interestingly, whereas the LT bands appeared at almost the same temperature range as for the fresh samples, the HT bands showed a flatter configuration and shifted to higher temperatures. This observation points out a dramatic change of the surface distribution of strong acid sites on the catalyst surface during the reaction, attaining a higher degree of heterogeneity. The LT and HT bands could be deconvoluted into 2 and 3 elementary bands, respectively. Weak and medium-strength bands (i.e. species I-III) were predominant for SBA@76 (Table 3).

The LT bands exhibited lower NH_3 loadings (Φ_{NH_3}) for the spent SBA@190 and SBA@102 compared to the parent catalysts, while almost equal loadings were measured for SBA@76 and SBA@27 (Table 2). These observations suggest that $\text{NH}_4^+ \cdot n\text{NH}_3$ associations could also be formed on weak acid sites for SBA@190 and SBA@102, providing in turn evidence for their Brønsted nature. Furthermore, the NH_3 loadings measured on the spent SBA@76, SBA@50 and SBA@27 catalysts could be safely used for estimating the acidity of weak acid sites. In the case of HT bands, these exhibited remarkably lower NH_3 loadings than for the parent catalysts, suggesting a minor formation degree of $\text{NH}_4^+ \cdot n\text{NH}_3$ associations ($n = 2.9$ for SBA@190, $n = 1.1$ for SBA@102 and SBA@76, $n = 0.3$ for SBA@27, Table 2). These results seem to indicate that partial hydrophobization of the catalysts due to coke formation can impact the distribution of strong acid sites, even after calcination at 500 °C.

Table 1. Textural properties of SBA@X before (BR) and after reaction (AR)^a

Sample	S_{BET} (m^2/g)		ΔS^c	V_g (cm^3/g)		D (nm)		Carbon (mg/g) ^d
	BR ^b	AR ^b		BR	AR	BR	AR	
SBA@250	688 (139)	363 (43)	47%	0.58	0.38	3.6	3.6	-
SBA@190	630 (123)	337 (27)	46%	0.61	0.34	3.6	3.3	86
SBA@102	611 (121)	339 (28)	46%	0.52	0.36	3.6	3.5	111
SBA@76	567 (126)	309 (22)	45%	0.57	0.36	3.9	4.0	112
SBA@50	524 (124)	292 (35)	44%	0.58	0.34	4.0	3.7	-
SBA@27	492 (103)	233 (39)	53%	0.55	0.26	4.1	3.8	119

^a Reaction conditions: 300 °C; ambient pressure; time on stream, 8 h; catalyst loading, 200 mg; 1,3-BDO flowrate, 2.8 mL/h; carrier N_2 flowrate, 60 mL(STP)/min

^b In parentheses, micropore surface areas

^c $\Delta S = [S_{\text{BET}}(\text{BR}) - S_{\text{BET}}(\text{AR})] / S_{\text{BET}}(\text{BR})$

^d Measured from TGA-MS in the range 300-680 °C

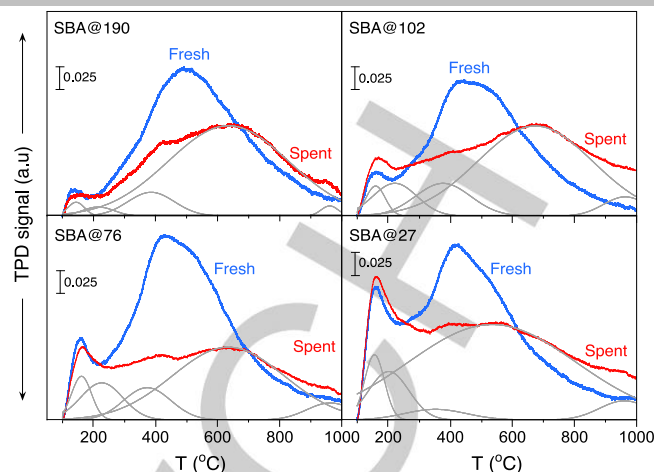


Figure 1. Normalized NH_3 -TPD profiles per weight of catalyst on 4 fresh (blue) and spent (red) SBA@X catalysts: SBA@190, SBA@102, SBA@76, SBA@27. The fresh and spent samples were calcined at 550 °C and 500 °C, respectively before the NH_3 -TPD profiles. The grey curves refer to distributions for the different acid sites in the spent samples measured after deconvolution (see detailed data in Table 3). The experimental conditions for TPD profiles can be found in the SI. Reaction conditions as in Table 1.

Table 2. Acidity of SBA@X catalysts measured from NH_3 -TPD and pyridine adsorption-IR

Catalyst	Al ($\mu\text{mol/g}$)	NH_3 uptake (Φ_{NH_3} , $\mu\text{mol/g}$) ^a		HT / (AI - LT)	B/L (Pyr)
		100-240 °C	240-1000 °C		
SBA@250	133	15 (-)	977 (-)	8.3 (-)	-
SBA@190	175	18 (10)	842 (485)	5.3 (2.9)	0.38
SBA@102	326	23 (12)	665 (339)	2.2 (1.1)	0.27
SBA@76	438	76 (77)	929 (400)	2.6 (1.1)	0.31
SBA@50	666	92 (-)	824 (-)	1.4 (-)	-
SBA@27	1233	186 (190)	854 (300)	0.8 (0.3)	0.28

^a In parentheses, NH_3 uptake measured on spent catalysts after calcination at 500 °C. Additional data can be found in Table S3.

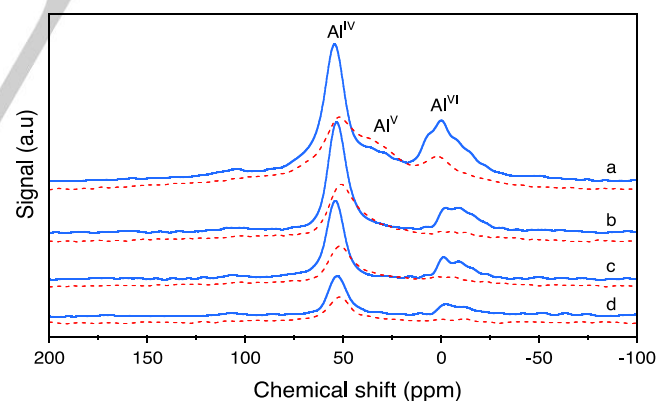


Figure 2. ^{27}Al -NMR MAS spectra on selected fresh SBA@X catalysts after calcination at 500 °C (a: SBA@27, b: SBA@76, c: SBA@102, d: SBA@190). Reaction conditions as in Table 1.

The nature of the acid sites in the fresh SBA@X catalysts was first assessed by pyridine adsorption-IR (Figure S5). All the samples showed two characteristic vibration bands centered at 1545 cm^{-1} and 1455 cm^{-1} that can be attributed to Brønsted (B) and Lewis (L) acid sites, respectively.^[22] Although the intensity of both bands increased with the $\text{SiO}_2/\text{Al}_2\text{O}_3$ ratio, the B/L ratio kept almost unchanged in the range 0.27-0.38 (Table 2). This picture is qualitative consistent with the ^{27}Al -NMR MAS spectra measured on the fresh samples (Figure 2). The spectra consisted of a main resonance bands centered at 55 ppm with a shoulder by

COMMUNICATION

WILEY-VCH

30 ppm, which is indicative of fourfold (Al^{IV} , framework) and fivefold (Al^{V} , ex-framework) coordinated species, respectively.^[21,23] A second band could be visualized at ca. 0 ppm that can be assigned to sixfold (Al^{VI} , ex-framework) coordinated species in either alumina-type phases or phases with ex-framework Al containing water molecules in the coordination sphere.^[21,23a]

A similar structural organization can be inferred from the ^{27}Al -NMR MAS spectra measured on the spent catalysts after calcination. The tetrahedral Al resonance band shifted to ca. 51 ppm with a slightly larger shoulder at 30 ppm (fivefold species). Unlike the fresh catalysts, this band showed a markedly lower intensity. This observation can be attributed to coke formation, altering the electronic atmosphere around the Al species.^[24] Moreover, the band centered at 0 ppm associated to sixfold coordinated Al species became very weak after reaction, which can be explained by either a partial removal or a transformation of Lewis acid sites (preferentially strong) into Brønsted acid sites with medium and strong strength in the presence of water.^[25] By comparing the ^{27}Al -NMR MAS spectra on the fresh and spent catalysts with the NH_3 -TPD profiles (Figure 1), we can attribute bands I-IV in the deconvoluted profiles to Brønsted acid species, whereas band V is expected to refer to strong and almost residual Lewis acid sites.

The catalytic performance of the SBA@X catalysts was assessed in the temperature range 200–300 °C at WHSV = 14 h⁻¹ (Tables S3–S5). In all cases, the main detected products were BD, propylene (PE) and 3-buten-1-ol (3B1ol), suggesting a reaction mechanism proceeding by a first dehydration step encompassing the formation of 3B1ol as main intermediate followed by two parallel reactions: (1) dehydration of 3B1ol into BD, and (2)

C-C cleavage of 3B1ol into PE. Heavy products might be further generated via PE and BD oligomerization, promoting coke formation. Minor byproducts were also detected including MEK, methyl vinyl ketone (MVK), 3-buten-2-ol (3B2ol), 1-butanol and 2-butanol. No ether formation was detected.^[26]

The catalytic stability was studied on stream over SBA@76 at 250 °C during 102 h (Figure 3). Full 1,3-BDO conversion was achieved during the initial 32 h followed by a slow deactivation to 82% after 102 h due to carbon deposition. In parallel, the BD yield declined slightly from 61% to 51% (the BD selectivity kept almost constant), giving rise to 3B1ol (increase from 0.5% to 11%), whereas the PE yield kept stable at around 20%. Noteworthy, the BD, PE and 3B1ol yields did not change appreciably during operation. These results suggest that the reaction mechanism was not altered during the dehydration reaction despite the loss of 1,3-BDO conversion. Furthermore, catalytic tests performed for a time on stream below 32 h ensured a proper measurement of the intrinsic catalytic activity.

Figure 4 and Figure S6 plot the main trends obtained for the 1,3-BDO conversion and the BD, PE and 3B1ol yields over the SBA@X catalysts, whereas Tables S6–S8 list the BD yields, BD/PE selectivity ratios and sum of selectivities (ΣS). The temperature favored PE formation instead of BD, suggesting a higher activation energy for PE generation from either 3B1ol or 3B2ol. In contrast, 3B1ol was promoted at lower temperatures, especially at lower $\text{SiO}_2/\text{Al}_2\text{O}_3$ ratios ($X=27$ –76). Furthermore, oligomerization was favored at lower temperatures. Overall, the best catalytic performance was achieved at 200 °C, affording BD/PE selectivity ratios in the range 3.3–4.5 for SBA@X catalysts ($X = 27$ –190) with moderate oligomerization ($\Sigma\text{S} = 72\%$ –84%).

Table 3. Deconvolution of LT and HT bands in the NH_3 -TPD profiles

Catalyst	Band I (LT)		Band II (LT)		Band III (HT)		Band IV (HT)		Band V (HT)	
	T_M (°C) ^a	Φ_{NH_3} (%)	T_M (°C) ^a	Φ_{NH_3} (%)	T_M (°C) ^a	Φ_{NH_3} (%)	T (°C) ^a	Φ_{NH_3} (%)	T (°C) ^a	Φ_{NH_3} (%)
SBA@190	144 (27)	3.9%	215 (51)	4.5%	386 (75)	13%	635 (194)	78%	961 (28)	0.13%
SBA@102	157 (31)	7.9%	219 (71)	18%	374 (89)	18%	671 (186)	55%	961 (70)	0.67%
SBA@76	159 (32)	12%	224 (68)	20%	371 (76)	16%	632 (180)	50%	960 (75)	0.70%
SBA@27	156 (32)	11%	202 (65)	15%	352 (100)	4.3%	535 (270)	69%	961 (80)	0.52%

^a T_M = mean temperature; in parentheses, standard deviation (also in °C).

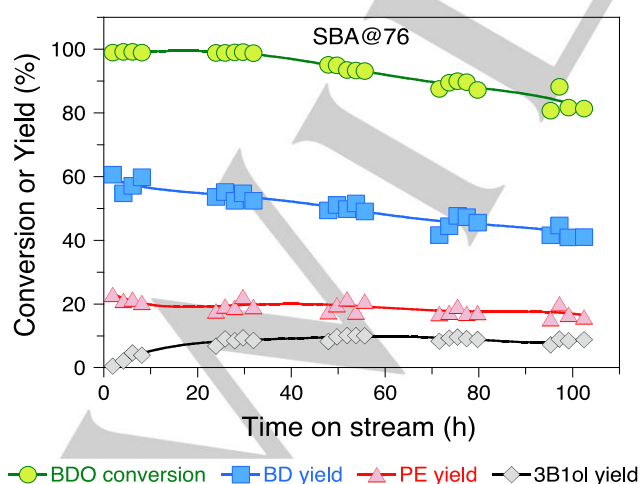


Figure 3. Catalytic stability of SBA@76 at 250 °C. Other detected products (<1% selectivity) include MEK, MVK, 1-butanol, 2-butanol and 3B2ol. Additional experimental conditions as in Table 1.

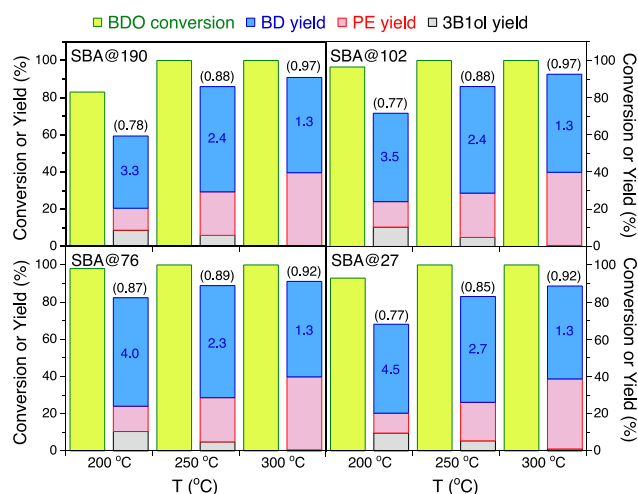


Figure 4. Influence of temperature on the catalytic performance of SBA@X catalysts for 1,3-BDO dehydration towards BD. Other detected products (<1% selectivity) include MEK, MVK, 1-butanol, 2-butanol and 3B2ol. Other reaction conditions as in Table 1. The numbers in the graphs indicate the BD/PE selectivity ratios (in blue) and the carbon balances (in parentheses).

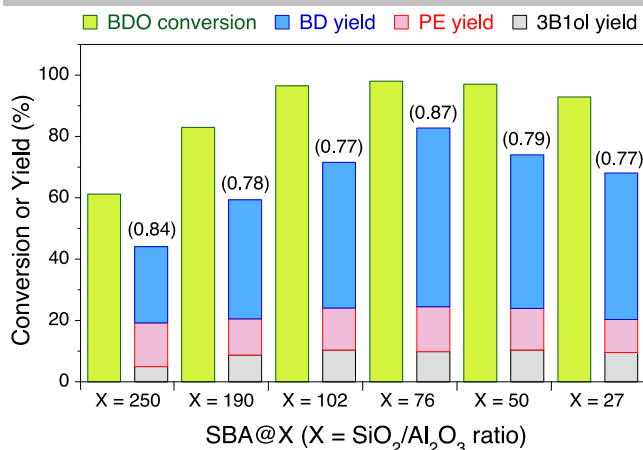


Figure 5. 1,3-BDO conversion and yield to main products (BD, PE, 3B1ol) over the SBA@X catalysts at 200 °C: SBA@250, SBA@190, SBA@102, SBA@76, SBA@50 and SBA@27. Other detected products (<1% selectivity) include MEK, MVK, 1-butanol, 2-butanol and 3B2ol. The numbers in parentheses on top of the yield bars indicate the carbon balance, whereas the numbers in parentheses in the abscissa axis indicate the density of weak acid sites on the fresh and spent samples expressed in $\mu\text{mol/g}$ (Table 2). Additional reaction conditions as in Table 1.

The catalytic performance of the SBA@X catalysts at 200 °C was very sensitive to the $\text{SiO}_2/\text{Al}_2\text{O}_3$ ratio (Figure 5). The 1,3-BDO conversion increased from 61% for SBA@250 to pass through a maximum at 98% for SBA@76, then dropped slightly to 93% for SBA@27. The maximum BD yield (59%) was achieved over SBA@76, resulting in a BD productivity as high as $4.9 \text{ g}_{\text{BD}} \cdot \text{g}_{\text{cat}}^{-1} \cdot \text{h}^{-1}$. Noteworthy, this productivity is about one order of magnitude higher than the that typically achieved in the Lebedev process (i.e. bioethanol \rightarrow BD), and 35% higher than that achieved on HZSM-5 catalysts ($\text{SiO}_2/\text{Al}_2\text{O}_3 = 260$).^[15] This enhanced catalytic properties over SBA@76 suggests that this catalyst presented an optimal distribution of acid sites for BD production. Since this catalyst was enriched in Brønsted acid sites with weak and medium strength, we can argue that these sites are responsible for 1,3-BDO dehydration into BD. These observations agree well with the conclusions drawn from earlier reports on 1-butanol and 1,3-BDO dehydration catalyzed by HZSM-5.^[15,27] Moreover, since a lower proportion of strong Brønsted acid sites (IV) was present in SBA@76 appearing at milder temperature unlike the other SBA@X catalysts, we can reasonably foresee a lower PL production by 1,3-BDO cracking.

In conclusion, an Al-SBA catalyst with an optimal $\text{SiO}_2/\text{Al}_2\text{O}_3$ ratio of 76 afforded a stable butadiene yield of 59% at a temperature as low as 200 °C in the gas-phase dehydration of 1,3-butanediol. The presence of native Brønsted acid sites with weak and medium strength was indispensable to achieve a high selectivity to butadiene as inferred from combined NH_3 -TPD, pyridine adsorption-IR, and ^{27}Al -NMR MAS. Carbon deposition over strong Lewis and Brønsted acid sites was unavoidable under the reaction conditions. As a result, a decrease of the surface area was observed together with a very moderate deactivation of the catalytic activity after 102 h operation at 250 °C.

Acknowledgements

Solvay is acknowledged for financial support. The REALCAT platform is also acknowledged for support in the XRF tests. The

REALCAT platform benefits from a government subvention administered by the French National Research Agency (ANR) within the frame of the 'Future Investments' program (PIA) with the contractual reference ANR-11-EQPX-0037. The Hauts-de-France Region and the FEDER as well as the Central Initiative Foundation are acknowledged for their financial contribution to the acquisition of the equipment of the platform. The authors would like to express their gratitude to V. Ruaux and M. Daturi for performing the pyridine adsorption-IR measurements.

Keywords

Keywords: Butadiene • 1,3-Butanediol • Dehydration • Acid catalysis • Al-SBA-15

- [1] A. J. Ragauskas, C. K. Williams, B. H. Davison, G. Britovsek, J. Cairney, C. A. Eckert, W. J. Frederick, J. P. Hallett, D. J. Leak, C. L. Liotta, J. R. Mielenz, R. Murphy, R. Templer, T. Tschaplinski, *Science* **2006**, *311*, 484-489.
- [2] a) N. Savage, *Nature* **2011**, *474*, S9-S11; b) J. R. Rostrup-Nielsen, *Science* **2005**, *308*, 1421-1422; c) A. Corma, S. Iborra, A. Velty, *Chem. Rev.* **2007**, *107*, 2411-2502; c) C. O. Tuck, E. Pérez, I. T. Horváth, R. A. Sheldon, M. Poliakoff, *Science* **2012**, *337*, 695-699.
- [3] a) Wm. Claude White, *Chem-Biol. Inter.* **2007**, *166*, 10-14; b) M. D. Jones, C. G. Keir, C. D. Iulio, R. A. M. Robertson, C. V. Williams, D. C. Apperley, *Catal. Sci. Technol.* **2011**, *1*, 267-272; b) E. V. Makshina, W. Janssens, B. F. Sels, P. A. Jacobs, *Catal. Today* **2012**, *198*, 338-344.
- [4] a) C. Angelici, B. M. Weckhuysen, P. C. A. Bruijninx, *ChemSusChem* **2013**, *6*, 1595-1614; b) H. M. Torres Galvis, K. P. de Jong, *ACS Catal.* **2013**, *3*, 2130-2149.
- [5] Z. Wang, in *Comprehensive Organic Name Reactions and Reagents*, John Wiley & Sons, Inc., **2010**, pp. 1728-1730.
- [6] a) M. Lewandowski, G. S. Babu, M. Vezzoli, M. D. Jones, R. E. Owen, D. Mattia, P. Plucinski, E. Mikolajska, A. Ochendusko, D. C. Apperley, *Catal. Commun.* **2014**, *49*, 25-28; b) C. Angelici, M. E. Z. Velthoen, B. M. Weckhuysen, P. C. A. Bruijninx, *ChemSusChem* **2014**, *7*, 2505-2515; c) C. Angelici, M. E. Z. Velthoen, B. M. Weckhuysen, P. C. A. Bruijninx, *Catal. Sci. Technol.* **2015**, *5*, 2869-2879; d) W. Janssens, E. V. Makshina, P. Vanelderden, F. De Clippel, K. Houthoofd, S. Kerkhofs, J. A. Martens, P. A. Jacobs, B. F. Sels, *ChemSusChem* **2015**, *8*, 994-1008; e) A. Chiericato, J. V. Ochoa, C. Bandinelli, G. Fornasari, F. Cavani, M. Mella, *ChemSusChem* **2015**, *8*, 377-388; f) O. V. Larina, P. I. Kyriienko, S. O. Soloviev, *Catal. Lett.* **2015**, *145*, 1162-1168.
- [7] V. L. Sushkevich, I. I. Ivanova, V. V. Ordonsky, E. Taarning, *ChemSusChem* **2014**, *7*, 2527-2536.
- [8] a) S. K. Bhattacharyya, S.K. Sanyal, *J. Catal.* **7** (1967) 152-158; b) G. O. Ezinkwo, V. F. Tretjakov, R. M. Talyshinky, A. M. Ilolov, T. A. Mutombo, *Catal. Commun.* **2014**, *43*, 207-212.
- [9] a) T. A. Werpy, J. E. Holladay, J. F. White, **2004**, pp. 1-67; b) N. Itoh, M. Nakamura, K. Inoue, Y. Makino, *Appl. Microbiol. Biotechnol.* **2007**, *75*, 1249-1256; c) X.-J. Ji, H. Huang, P.-K. Ouyang, *Biotechnol. Adv.* **2011**, *29*, 351-364; d) H. Yim, R. Haselbeck, W. Niu, C. Pujol-Baxley, A. Burgard, J. Boldt, J. Khandurina, J. D. Trawick, R. E. Osterhout, R. Stephen, J. Estadilla, S. Teisan, H. Brett Schreyer, S. Andrae, T. H. Yang, S. Y. Lee, M. J. Burk, S. van Dien, *Nat. Chem. Biol.* **2011**, *7*, 445-452; e) N. Kataoka, A. S. Vangnai, T. Tajima, Y. Nakashimada, J. Kato, *J. Biosci. Bioeng.* **2013**, *115*, 475-480; f) J. Baek, T. Y. Kim, W. Kim, W. Kim, H. J. Lee, J. Yi, *Green Chem.* **2014**, *16*, 3501-3507.
- [10] H. Duan, Y. Yamada, S. Sato, *Chem. Lett.* **2016**, *45*, 1036-1047.
- [11] L. Ott, S. Kohl, M. Bicker, H. Vogel, *Chem. Eng. Technol.* **2005**, *28*, 1561-1568.
- [12] a) H. Gotoh, Y. Yamada, S. Sato, *Appl. Catal. A: Gen* **2010**, *377*, 92-98; b) S. Sato, F. Sato, H. Gotoh, Y. Yamada, *ACS Catal.* **2013**, *3*, 721-734; c) V. K. Díez, P. A. Torresi, P. J. Luggren, C. A. Ferretti, J. I. Di Cosimo, *Catal. Today* **2013**, *213*, 18-24; d) R. Takahashi, T. Sodesawa, N. Yamamoto, *Catal. Commun.* **2004**, *5*, 397-400; e) N. Yamamoto, S. Sato, R. Takahashi, K. Inui, *Catal. Commun.* **2005**, *6*, 480-484; f) N. Ichikawa, S. Sato, R. Takahashi, T. Sodesawa, *J. Mol. Catal. A: Chem.*

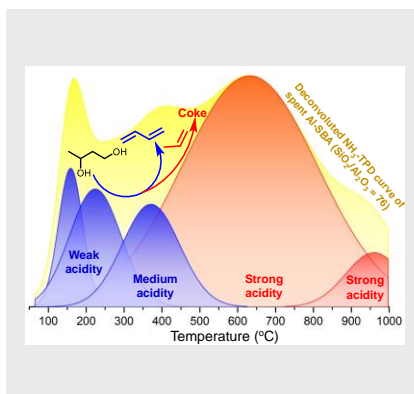
- 2006, 256, 106-112; g) F. Sato, S. Sato, Y. Yamada, M. Nakamura, A. Shiga, *Catal. Today* **2014**, 226, 124-133.
- [13] a) H. Duan, D. Sun, Y. Yamada, S. Sato, *Catal. Commun.* **2014**, 48, 1-4; b) H. Duan, Y. Yamada, S. Sato, *Appl. Catal. A: Gen.* **2015**, 491, 163-169.
- [14] a) W. Zhang, D. Yu, X. Ji, H. Huang, *Green Chem.* **2012**, 14, 3441-3450; b) A. Multer, N. McGraw, K. Hohn, P. Vadlani, *Ind. Eng. Chem. Res.* **2013**, 52, 56-60.
- [15] F. Jing, B. Katryniok, M. Araque, R. Wojcieszak, M. Capron, S. Paul, M. Daturi, J.-M. Clacens, F. De Campo, A. Liebens, F. Dumeignil, M. Peratitus, *Catal. Sci. Technol.* **2016**, 6, 5830-5840.
- [16] a) M. Caillot, A. Chaumonnot, M. Digne, J. A. van Bokhoven, *J. Catal.* **2014**, 316, 47-56; b) A. Corma, *Chem. Rev.* **1995**, 95, 559-614.
- [17] a) K. S. W. Sing, D. H. Everett, R. A. W. Haul, L. Moscou, R. A. Pierotti, J. Rouquerol, T. Siemieniewska, *Pure Appl. Chem.* **1985**, 57, 603-619; b) A. Neimark, K. S. W. Sing, M. Thommes in *Surface Area and Porosity* (Eds.: G. Ertl, H. Knözinger, F. Schüth, J. Weitkamp), 2nd edition, Verlag Chemie, **2008**; c) M. Thommes, *Physical Adsorption Characterization of Ordered and Amorphous Mesoporous Materials*, in *Nanoporous Materials: Science and Engineering* (Eds.: G. Q. Lu, X. S. Zhao), Imperial College Press, Oxford, **2004**; d) K. S. W. Singh, R. T. Williams, *Ads. Sci. Technol.* **2004**, 22, 773-782.
- [18] a) S. Wu, J. Huang, T. Wu, K. Song, H. Wang, L. Xing, H. Xu, L. Xu, J. Guan, Q. Kan, *Chin. J. Catal.* **2006**, 27, 9-14; b) T. Jiang, H. Tao, J. Ren, X. Liu, Y. Wang, G. Lu, *Micropor. Mesopor. Mater.* **2011**, 142, 341-346.
- [19] N. Lucas, G. Kokate, A. Nagpure, S. Chilukuri, *Micropor. Mesopor. Mater.* **2013**, 181, 28-46.
- [20] F. Lónyi, J. Valyon, *Micropor. Mesopor. Mater.* **2001**, 47, 293.
- [21] A. J. J. Koekkoek, J. A. R. van Veen, P. B. Gerttisen, P. Giltay, P. C. M. M. Magusin, E. J. M. Hensen, *Micropor. Mesopor. Mater.* **2012**, 151, 34-43.
- [22] a) L. G. Possato, R. N. Diniz, T. Garetto, S. H. Pulcinelli, C. V. Santilli, L. Martins, *J. Catal.* **2013**, 300, 102-112; b) P. A. Russo, M. M. Antunes, P. Neves, P. V. Wiper, E. Fazio, F. Neri, F. Barreca, L. Mafra, M. Pillinger, N. Pinna, A. A. Valente, *Green Chem.* **2014**, 16, 4292-4305; c) K. K. Ramasamy, M. A. Gerber, M. Flake, H. Zhang, Y. Wang, *Green Chem.* **2014**, 16, 748-760.
- [23] a) W. Hu, Q. Luo, Y. Su, L. Chen, Y. Yue, C. Ye, F. Deng, *Micropor. Mesopor. Mater.* **2006**, 92, 22-30; b) E. J. M. Hensen, D. G. Poduval, P. C. M. M. Magusin, A. E. Coumans, J. A. R. van Veen, *J. Catal.* **2010**, 269, 201-218.
- [24] R. H. Meinhold, D. M. Bibby, *Zeolites* **1990**, 10, 146.
- [25] a) D. P. Serrano, R. A. García, G. Vicente, M. Linares, D. Procházková, J. Čejka, *J. Catal.* **2011**, 279, 366-380; b) A. Ungureanu, B. Dragoi, V. Hulea, T. Cacciaguerra, D. Meloni, V. Solinas, E. Dumitriu, *Micropor. Mesopor. Mater.* **2012**, 163, 51-64; c) W. Zhu, H. Yang, J. Chen, C. Chen, L. Guo, H. Gan, X. Zhao, Z. Hou, *Green Chem.* **2014**, 16, 1534-1542.
- [26] a) B. Katryniok, S. Paul, M. Capron, C. Lancelot, V. Bellière-Baca, P. Rey, F. Dumeignil, *Green Chem.* **2010**, 12, 1922-1925; b) F. Secundo, G. Roda, M. Vittorini, A. Ungureanu, B. Dragoi, E. Dumitriu, *J. Mater. Chem.* **2011**, 21, 15619-15628.
- [27] H. Vinek, J. A. Lercher, H. Noller, *J. Molec. Catal.* **1985**, 30, 353-359.

Entry for the Table of Contents (Please choose one layout)

Layout 1:

COMMUNICATION

An Al-SBA-15 catalyst with a silica/alumina ratio of 76 was very active and selective for the production of butadiene by dehydration of 1,3-butane-diol at 200 °C due to the generation of a family of Brønsted acid sites of weak and medium strength during reaction.



Fangli Jing, Benjamin Katryniok, Sébastien Paul, Lin Fang, Armin Liebens, Ming Shen, Bingwen Hu, Franck Dumeignil and Marc Pera-Titus

Page No. – Page No.

Al-doped SBA-15 catalysts for low-temperature dehydration of 1,3-butane-diol into butadiene